# A Wideband Frequency-Selective Rasorber Based on Interdigital Resonator and Fractal Shaped Slot

Ying Sun, Shaoqiu Xiao, Zhixin Yao, Qi Shi
School of Physics, University of Electronic Science and Technology of China
Chengdu, China
15282280778@163.com; xiaoshaoqiu@uestc.edu.cn

***Abstract*— A two-layer design which has a wideband transmission window within an ultra-wide absorption band, named as frequency-selective rasorber (FSR), is presented. This structure enables small insertion loss in the wide transmission window, with two absorption bands below and above the passband. The equivalent circuit (EC) is employed to make the design clearer and straightforward. Compared with other FSRs, it has a much wider transmission band with an ultra-wide absorption band and relative low profile. The simulated results exhibit that the insertion loss is less than 3 dB from 9.59 to 12.16 GHz (23.6%), while the frequency for −10dB reflection coefficient ranges from 5.4 to 17GHz (103.6%) with a thickness of 0.106$\lambda_L$ ($\lambda_L$ is wavelength at the lowest working frequency).**

***Index Terms*—Absorption, frequency-selective rasorber (FSR), interdigital resonator (IR), transmission, circuit analog absorber.**

## I. Introduction

Bandpass frequency selective surface (FSS) has been widely applied in military radar antenna systems. It can transmit electromagnetic (EM) waves with low insertion loss in a certain frequency band, but produces very large reflection outside the passband. In order to improve the stealth performance of radar antennas, the design of bandpass FSS with reduced reflection from the rejection bands attracts more and more attention [1]. Absorbers which can absorb most of the incident wave shall be a very useful method to solve the problem. The final structure that implements this function is radar absorbers with a transmission window, academically called frequency selective rasorber (FSR), where the "rasorber" is a combination of "radome" and "absorber" [2].

For these reported rasorber designs, Munk is the first researcher who proposed a new absorbing radome structure with passband performance through circuit analog absorber (CAA) and the frequency selective surface, which promotes the development of the technology[2]. Later, Costa [3], Motevasselian [4] and Qiang Chen [5] employ different methods to improve the transmission or absorption performance. Existing FSR is divided into 2-D FSR and 3-D FSR according to their respective structures. 2-D FSRs are composed by cascading resistors and bandpass FSS [3]–[4], [6]–[11]. 3-D FSRs typically have several multimode cavities based on parallel plate waveguides that produce multimode resonators of several different frequencies, including lossless resonators at the passband and lossy resonators at the absorption band [12]. However, there are two problems from the above mentioned FSR structures, which have not been completely solved yet. 1) The

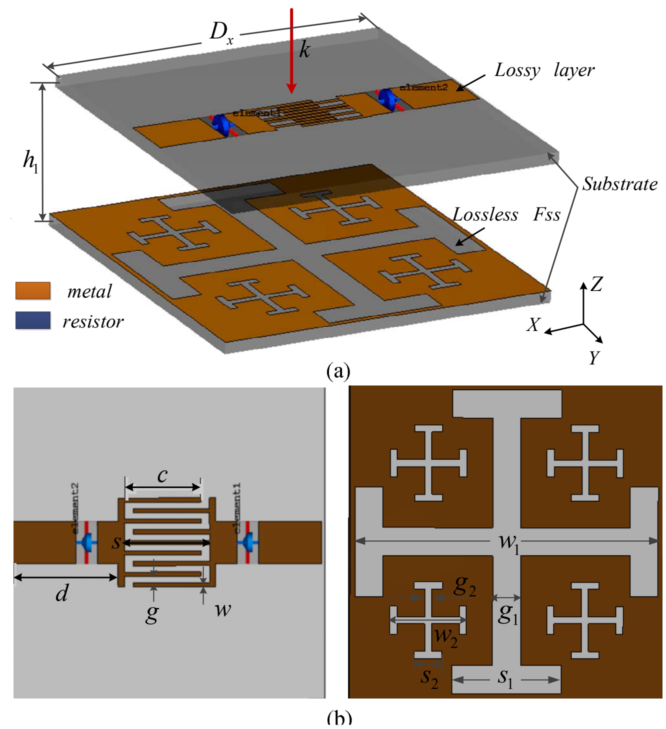


Fig. 1. (a) Perspective view of the unit cell structure of the proposed rasorber. (b) Top view of the lossy layer and lossless FSS unit cells

transmission bandwidth in the reported literature is very narrow, just about 4% [5]; 2) The absorbing bandwidth of the structure is narrow and the absorbing ability to the incident electromagnetic wave is weak.

In this article, in order to increase the passband bandwidth and improve the absorption bandwidth in the low and high frequency bands, a new 2-D FSR is introduced. Based on the equivalent circuit model (ECM), optimization algorithm and simulation software, the restrictive condition of the equivalent impedance of the lossy and lossless layer are theoretically analyzed. The new structure designs in this article greatly expands the transmission bandwidth (23.6%) and the absorbing bandwidth (the frequency range of the reflection coefficient below −10 dB is achieved from 5.4 to 17 GHz).

978-1-7281-0716-5/19/$31.00 ©2019 IEEE

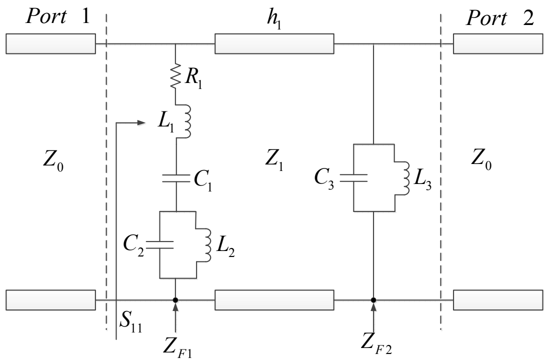


Fig. 2. Equivalent circuit model of FSR

## II. FSR Design and Simulation

### A. FSR Structure and Equivalent Circuit

As shown in Fig. 1, the FSR consists of a lossy layer and a lossless layer. The lossy layer is composed of an interdigitated metal strip loaded with two resistor elements which is supported by a thin substrate. Most incident EM wave shall be absorbed by the resistors when the layer resonates. The lossless layer, made of slot dipoles of different sizes printed on the same substrate, behaves as a bandpass FSS. Slot dipoles of different sizes shall slow down the rising speed of insertion loss away from the resonant frequency, and thus effectively expand the passband bandwidth. The space between the two layers are filled with air and the distance is $h_1$.The substrate thickness and relative dielectric constant are respectively $d = 0.254$ mm, $\varepsilon_r = 3.48$.

Equivalent circuit is an effective method to analyze FSR in recent years [8]. The equivalent circuit of FSR designed in this article is shown in Fig. 2. According to [1], the interdigitated metal strip can be equivalent to a parallel *LC* circuit, where the inductance is realized by a metal strip connecting the two separated portions, and the capacitance is realized by the mutual coupling between the fingers. The series *RLC* circuit represents the lumped resistors and two short-circuit arms on both sides of the interdigitated metal strip. $R_1$, $L_1$, $C_1$ and $L_2$, $C_2$ are determined by the lossy layer, while $L_3$, $C_3$ are determined by the lossless frequency selective surface, and the value of the lumped element can be derived from the formulas in [5]. The incident and transmitted space are equivalent to port 1 and port 2, respectively.

According to the equivalent circuit model of FSR shown in the Fig. 2, the ABCD matrix of the network is written as

$$\begin{bmatrix} A & B \\ C & D \end{bmatrix} = \begin{bmatrix} 1 & 0 \\ Y_{F1} & 1 \end{bmatrix} \begin{bmatrix} \cos\theta_1 & jZ_1 \sin\theta_1 \\ jY_1 \sin\theta_1 & \cos\theta_1 \end{bmatrix} \begin{bmatrix} 1 & 0 \\ Y_{F2} & 1 \end{bmatrix} \tag{1}$$

Where $Y_{F1}=1/Z_{F1}$, $Y_1=1/Z_1$, $Y_{F2}=1/Z_{F2}$, $\theta_1 = 2\pi f h_1 \sqrt{\varepsilon_r} / c$ , $f$ is the operating frequency and $c$ is the speed of light in vacuum. Then using the conversion between ABCD matrix and S matrix [1], the expressions for $S_{11}$ and $S_{21}$ can be obtained as,

$$|s_{11}| = \left| \frac{A + \frac{B}{Z_0} - CZ_0 - D}{A + \frac{B}{Z_0} + CZ_0 + D} \right| = \frac{j\left(\frac{Z_1}{Z_0} - \frac{Z_0}{Z_1}\right)N - \frac{Z_0(M)}{\tan\theta_1} + jZ_1(Z_{F1} - Z_0 - Z_{F2})}{j\left(\frac{Z_1}{Z_0} + \frac{Z_0}{Z_1}\right)N + \frac{2N + Z_0(M)}{\tan\theta_1} + jZ_1(M + Z_0)} \tag{2}$$

$$|S_{21}| = \left| \frac{2}{A + \frac{B}{Z_0} + CZ_0 + D} \right| = \frac{2Z_1 N}{\left(2N + Z_0(M)\right) Z_1 \cos\theta_1 + \left(PN + Z_1^2 \left(Z_0 + M\right)\right) j \sin\theta_1} \tag{3}$$

Where $M = Z_{F1} + Z_{F2}$, $N = Z_{F1} Z_{F2}$, $P = Z_1^2 / Z_0 + Z_0$ .

The principle of this work can be clearly known according to the equivalent circuit model, assuming

$$f_1 = \frac{1}{2\pi\sqrt{L_1 C_1}}, f_2 = \frac{1}{2\pi\sqrt{L_2 C_2}}, f_3 = \frac{1}{2\pi\sqrt{L_3 C_3}}, \qquad f_1 \langle f_2 = f_3 \tag{4}$$

1) When the operation frequency $f < f_1$, the impedance of series $L_1$, $C_1$ is capacitive while the impedance of parallel $L_2$, $C_2$ is inductive. So there is a frequency $f = F_1$ which makes the imaginary part of $Z_{F1}$ 0, and produces a resonance. At the resonant frequency $F_1$, the lossless layer can be regarded as a PEC, so the electromagnetic waves are all reflected, with no wave passing through. The whole structure works as a CAA, and most energy is absorbed by the resistors $R$ in the lossy layer. Thus the structure has a strong performance of absorption at $F_1$.
2) When the operating frequency is $f_2$, Since $f_2$ is the resonate frequency of $L_2$, $C_2$, the impedance of parallel $L_2$, $C_2$ is infinite, the impedances of other components of this branch can be neglected, that is, $Z_{F1} = \infty$. Thus, the loss layer can achieve full wave transmission. Similarly, the impedance of $L_3$, $C_3$ is also infinite at $f_2$, so $Z_{F2} = \infty$. Therefore, the structure can achieve full wave transmission at $f_2$, and the insertion loss is smallest.
3) When the operation frequency $f > f_2$, the impedance of series $L_1$, $C_1$ is inductive while the impedance of parallel $L_2$, $C_2$ is capacitive. So, there is a frequency $f = F_2$ which makes the imaginary part of $Z_{F1}$ 0, and produces a resonance. At the resonant frequency $F_2$, the lossless layer can be regarded as a PEC, so the electromagnetic waves are all reflected, with no wave passing through. The whole structure works as a CAA, and most energy is absorbed by the resistors $R$ in the lossy layer. Thus the structure has a strong performance of absorption at $F_2$

### B. Optimization Algorithm to Determine Structural Parameters

According to the formulas (1)–(3), the value of reflection and transmission coefficient can be quickly calculated. Therefore, this article uses Differential Evolution (DE) to optimize the structure parameters shown in Fig. 1 and $|S_{11}| < -10$ dB as

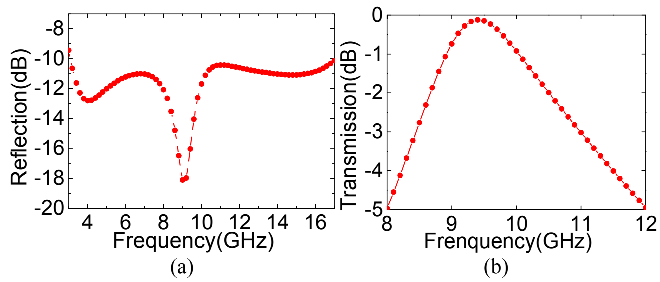


Fig. 3. (a) Optimal reflection coefficient curve based on equivalent circuit model. (b) Optimal transmission coeff cient curve based on equivalent circuit model.

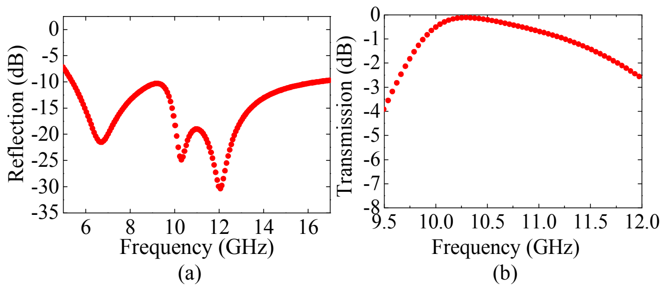


Fig. 4. (a) Simulated ref ection coeff cients of FSR. (b) Simulated transmission coeff cients of FSR

the objective function. The result of obtaining parameters is:

$$D_x = 7.3\text{mm}, h_1 = 5.2\text{mm}, c = 1.42\text{mm}, s = 2.1\text{mm}, d = 2.4\text{mm},$$
$$g = 0.1\text{mm}, w = 0.1\text{mm}, w_1 = 7\text{mm}, w_2 = 1.1\text{mm}, g_1 = 0.5\text{mm},$$
$$g_2 = 0.05\text{mm},\ s_1 = 2.5\text{mm},\ s_2 = 0.6\text{mm}$$

The reflection coefficient curve and the transmission curve are shown in Fig. 3. As can be seen from Fig. 3, the reflection coefficient is less than -10 dB in the frequency range of 3 to 17 GHz (140%), and the overall profile is only 0.103 $\lambda_L$. The transmission curve is less than −3 dB at 8.4-11 GHz. So in theory the structure can broaden the transmission and absorption bandwidth.

### *C. Simulation Optimization*

In the low frequency band, since $h_1$ is much smaller than the wavelength, there is an equivalent capacitance between the lossy layer and the lossless layer, so the circuit of Fig. 2 cannot be accurately equivalent to the model of Fig. 1 in the entire absorbing band. The reflection coefficient result in Fig. 3 has a certain error compared with the actual result. Therefore, it is necessary to improve the parameters using simulation software. In this article, CST is used to further optimize. The infinite array is simulated using periodic boundary conditions, and the Floquet port is placed directly above to simulate plane-wave incidence. The final parameter results of the optimization are shown in Fig. 4.

The simulation results obtained under normal incidence are shown in Fig. 4. It can be seen that the 10dB absorbing bandwidth of the FSR structure is 103.6% (5.4~17GHz), and the total height of the model is 0.106 $\lambda_L$. The bandwidth for 3dB transmission coefficient is 23.6% (9.59-12.16GHz), which is significantly expanded and meets the design requirements.

## III. Conclusion

In this article, a wideband frequency selective rasorber based on interdigital resonator and fractal shaped slot is proposed. The band with $|S_{11}| < -10$ dB spans from 5.4 to 17 GHz, a passband can be obtained at 10.28 GHz with an insertion loss of only 0.118 dB. What's more, the bandwidth of -3dB transmission coefficient is 23.6% (9.59-12.16GHz), which is the widest to the author's best knowledge. The absorption and transmission bands include most of the S-band and the C, X, and Ku bands, which has high application prospects.

## Acknowledgment

This work was supported in part by National Natural Science Foundation of China (61731005), in part by the Pre-Research Project (41413060404), and in part by the Fundamental Research Funds for the Central Universities (ZYGX2016Z008).

## References

[1] Y. Shang, Z. Shen and S. Xiao, "Frequency-Selective rasorber based on square-loop and cross-dipole arrays," *IEEE Trans. Antennas Propag.,* vol. 62, no. 11, pp. 5581-5589, Nov. 2014.

[2] B. A. Munk, Metamaterials: *Critique and Alternatives*. Hoboken, NJ, USA: Wiley, 2009.

[3] F. Costa and A.Monorchio. "A frequency selective radome with wideband absorbing properties," *IEEE Trans. Antennas Propag.,* vol. 60, no. 6, pp. 2740–2747, Jun. 2012.

[4] A. Motevasselian and B. L. G. Jonsson. "Design of a wideband rasorber with a polarization-sensitive transparent window," *IET Microw. Antennas Propag,* vol. 6, no. 7, pp. 747–755, 2012.

[5] Q. Chen, D. Sang, M. Guo, and Y. Fu, "Frequency-Selective rasorber with interabsorption band transparent window and interdigital resonator," *IEEE Trans Antennas Propag.*, vol. 66, no. 8, pp. 4105-4114, Aug. 2018.

[6] L. Liu et al., "Design of an invisible radome by metamaterial absorbers loaded with lumped resistors," *Chin. Phys. Lett.,* vol. 30, no. 6, 2013.

[7] Q. Chen, J. J. Bai, L. Chen, and Y. Q. Fu, "A miniaturized absorptive frequency selective surface," *IEEE Antennas Wireless Propag. Lett.*, vol. 14, pp. 80–83, 2015.

[8] X. Chen, Y. Li, Y. Fu, and N. Yuan, "Design and analysis of lumped resistor loaded metamaterial absorber with transmission band," *Opt. Exp.,* vol. 20, no. 27, pp. 28347–28352, 2012.

[9] Q. Chen, L. Chen, J. Bai, and Y. Fu, "Design of absorptive frequency selective surface with good transmission at high frequency," *Electron. Lett.*, vol. 51, no. 12, pp. 885–886, Jun. 2015.

[10] K. Zhang, W. Jiang, and S. Gong, "Design bandpass frequency selective surface absorber using LC resonators," *IEEE Antennas Wireless Propag. Lett.*, vol. 16, pp. 2586–2589, 2017.

[11] Y. Han, W. Che, X. Xiu, W. Yang, and C. Christopoulos, "Switchable low-prof le broadband frequency-selective rasorber/absorber based on slot arrays," *IEEE Trans. Antennas Propag.,* vol. 65, no. 12, pp. 6998–7008, Dec. 2017.

[12] Y. Yu, Z. Shen, T. Deng, and G. Luo, "3-D frequency-selective rasorber with wide upper absorption band," *IEEE Trans. Antennas Propag.,* vol. 65, no. 8, pp. 4363–4367, Aug. 2017.